Supporting Information

Synthesis of Co-based bimetallic nanocrystals with one-dimensional structure for selective control on syngas conversion

Rongbin Ba,[a,b] Yonghui Zhao,[a] Lujing Yu,[a,b] Jianjun Song,[a,b] Shuangshuang Huang,[a,b]

Liangshu Zhong,[a] Yuhan Sun,*[,a,c] and Yan Zhu*[, a,c]

[a] CAS Key Laboratory of Low-Carbon Conversion Science and Engineering, Shanghai Advanced Research Institute, Chinese Academy of Sciences, Shanghai 201210, China
[b] University of Chinese Academy of Sciences, Beijing, 100049, China
[c] School of Physical Science and Technology, ShanghaiTech University, Shanghai 201210, China

Supporting Figures

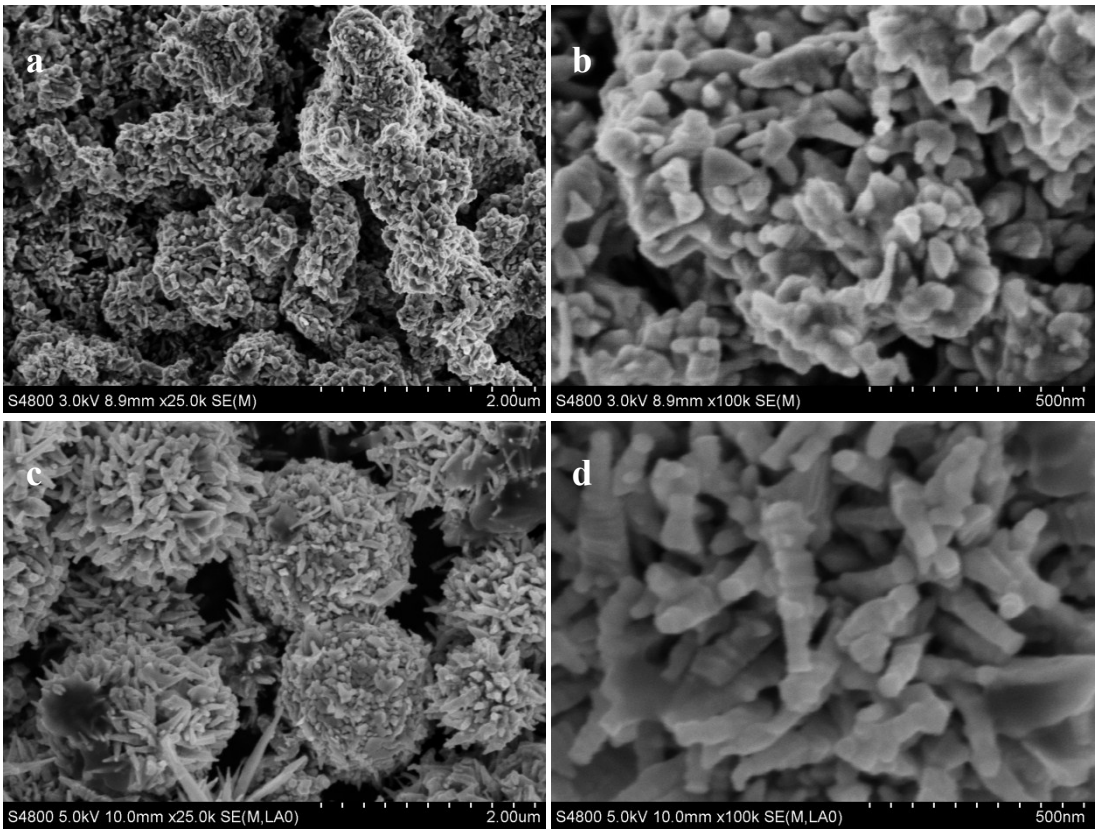

Figure S1. (a) and (b) SEM images of Co nanocrystals synthesized in propylene glycol solvent with stearic acid as a surfactant at 190°C for 5h without Pd as seeds. (c) and (d) SEM images of

Co nanocrystals synthesized in propylene glycol solvent with stearic acid and hexadecylamine as double surfactants at 160^{o}C for 15h without Cu as seeds.

No introducing surfactant in the synthesis route, there are no slim peripheral branches of Co-Pd particles, and big lumps onto the shell surface can be found (Figure S2a). The optimum concentration of stearic acid should be 0.05 mol/L, and the rod-like branches are much slim in contrast to high or low content of stearic acid (Figure S2b-e). Besides stearic acid as a surfactant to promote the whisker growth of Co-Pd, oleic acid can also play a similar role on assisting one-sided growth of Co-based nanocrystals (Figure S2f). Next, the structure and component of Co-Pd bimetal are related with the reaction time and reaction temperature.If the reaction time was more than 5 h, the length of peripheral branches would become shorter (Figure S3c). Reaction temperatures also need taking into account for controlling the shape of Co-Pd nanocrystals, where the optimum temperature was 190^{o}C. When reaction temperature was lower than 190^{o}C, with the temperature decrease, peripheral branches became short, while the reaction temperature was higher than 190^{o}C such as 210^{o}C for 5h, peripheral branches were short (Figure S3a, b, and d). Figure S3e-j show the shape evolution of Co-Pd nanocrystals at different stage. When the synthesis was conducted for 1h, cobalt stearate was formed (2θ=21.5°) and no CoPd nanostystal was formed, as shown in Figure S4. Carboxyl is electrophilic group which can provide electron cloud to Co^{2+} to form coordinate bond, leading to the decrease of Co^{2+} in the solution. When the reaction proceed to 2h, CoPd nanocrystals started to form and the cobalt stearate started to consume, which was coincident with the diffraction peaks at 2h. When the reaction time was up to 3h, the cobalt nearly exhaused and most of CoPd nanocrystals formed although their construction were not uniform. Until to 3.5h, the cobalt stearate were completely consumed, indicated by XRD studied.

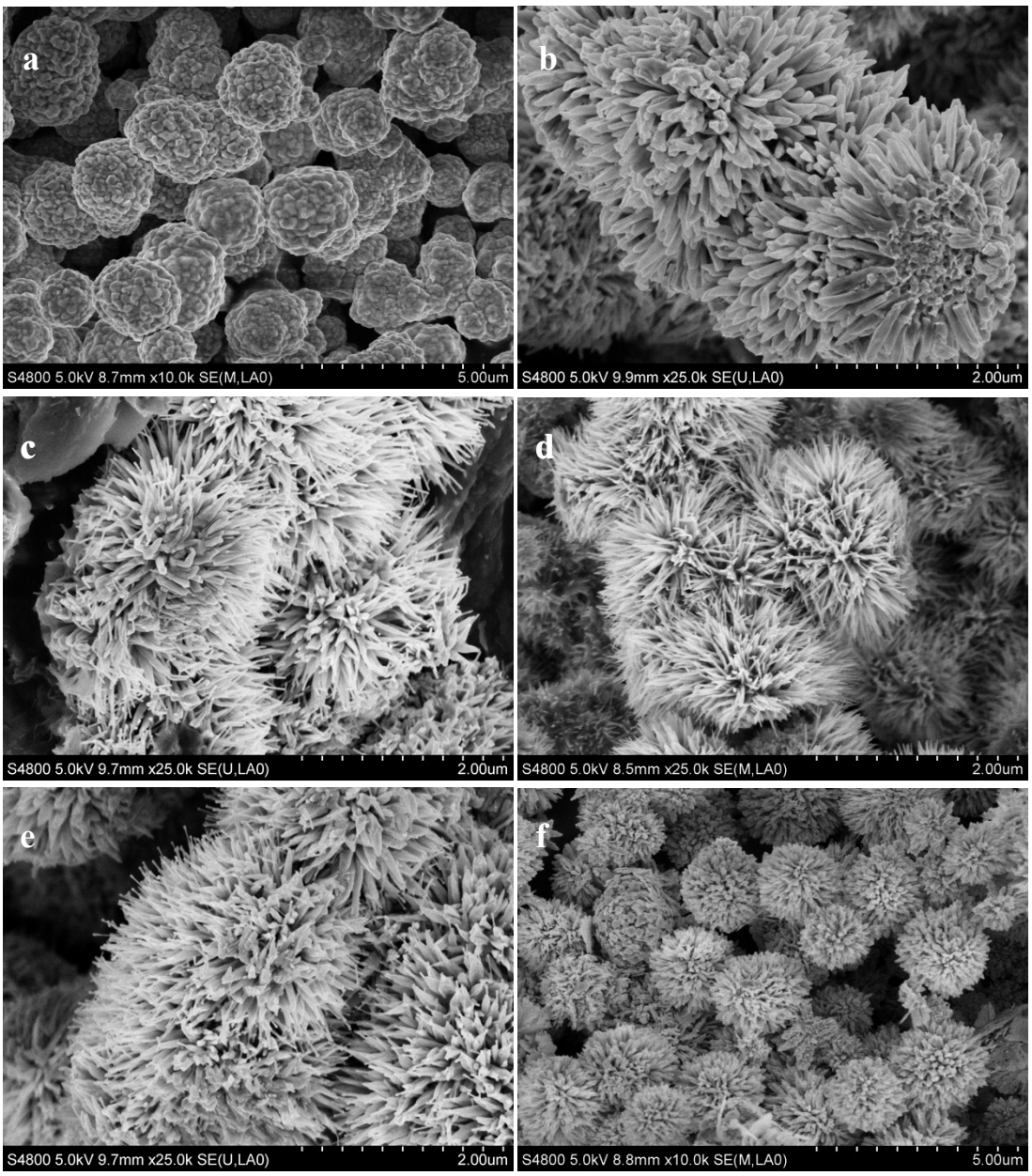

Figure S2. SEM images of $CoPd_{0.001}$ nanocrystals synthesized at 190°C (a) without surfactants, (b) 0.0125 mol/L stearic acid, (c) 0.025 mol/L stearic acid, (d) 0.05 mol/L stearic acid, (e) 0.1 mol/L stearic acid, and (f) using 0.05 mol/L oleic acid as a surfactant, respectively.

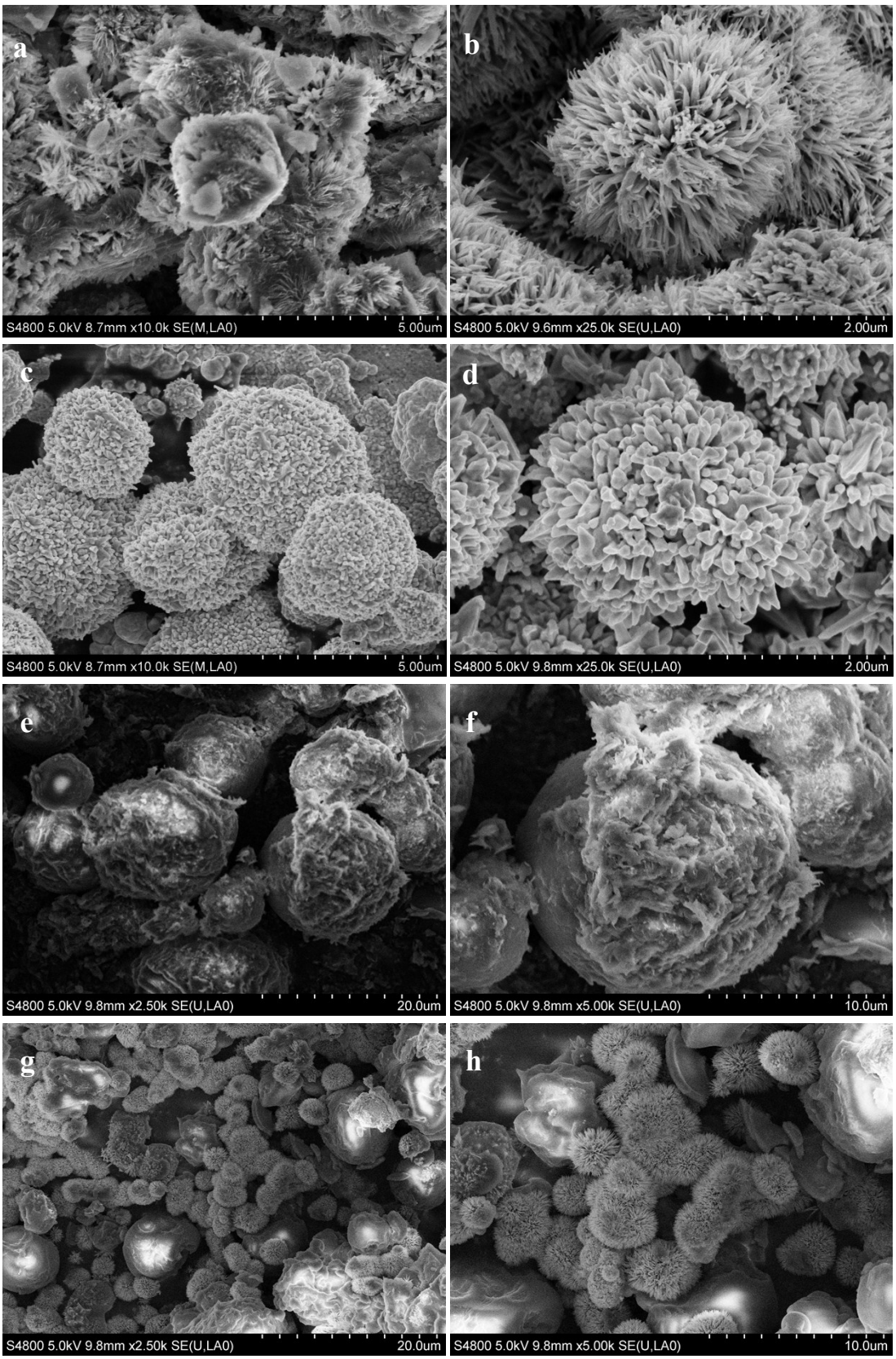
a
S4800 5.0kV 8.7mm x10.0k SE(M,LA0)
5.00um
b
S4800 5.0kV 9.6mm x25.0k SE(U,LA0)
2.00um
c
S4800 5.0kV 8.7mm x10.0k SE(M,LA0)
5.00um
d
S4800 5.0kV 9.8mm x25.0k SE(U,LA0)
2.00um
e
S4800 5.0kV 9.8mm x2.50k SE(U,LA0)
20.0um
f
S4800 5.0kV 9.8mm x5.00k SE(U,LA0)
10.0um
g
S4800 5.0kV 9.8mm x2.50k SE(U,LA0)
20.0um
h
S4800 5.0kV 9.8mm x5.00k SE(U,LA0)
10.0um

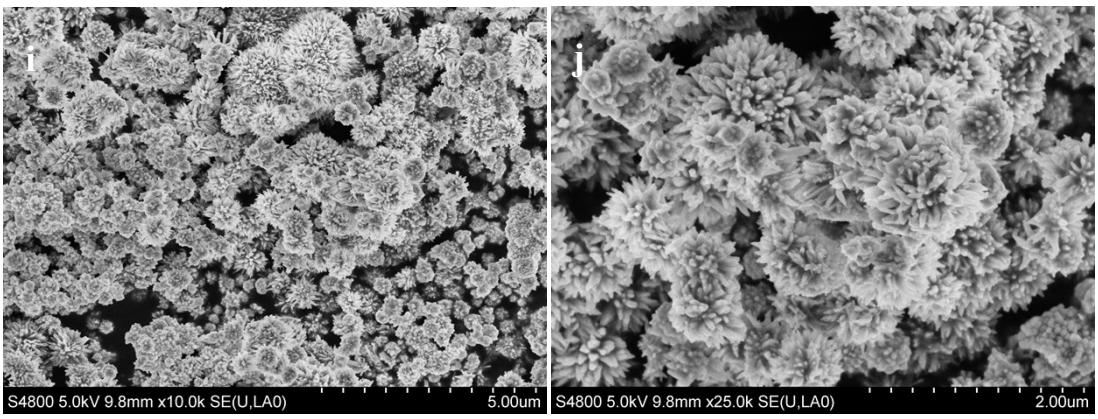

Figure S3. (a) SEM image of $CoPd_{0.001}$ nanocrystals synthesized at 150°C for 5h. (b) SEM image of $CoPd_{0.001}$ nanocrystals synthesized at 170°C for 5h. (c) SEM image of $CoPd_{0.001}$ nanocrystals synthesized at 190°C for 15h. (d) SEM image of $CoPd_{0.001}$ nanocrystals synthesized at 210°C for 5h. SEM image of $CoPd_{0.001}$ nanocrystals synthesized at 190°C for (e, f) 1h, (g, h) 2h, and (i, j) 3h, respectively.

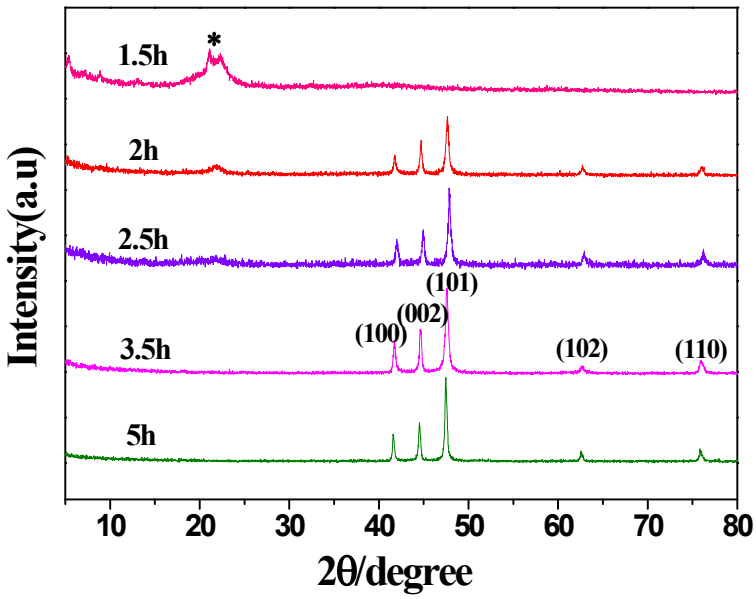

Figure S4. XRD patterns of Co-based (Co-Pd) nanocrystals synthesized at 190 °C for different reaction time (asterisk for cobalt stearate).

Long-chain carboxylic acid and long-chain amine such as stearic acid and hexadecylamineas a pair of ligands play a key role on shaping thedendrite-like structure of Co-Cu bimetallic nanocrystals. If only stearic acid was used as a surfactant, although the 3D core-shell structure of Co-Cu can be also obtained, the size of core is larger than 500 nm and therod-like branches on the shell are too short. With the increase of Cu content, the length of peripheral branches got shorter and solid core became larger (Figure S5a-c). Especially, the length of rods of $CoCu_{0.2}$ (20wt% Cu) is nearly negligibleand the cores are up to micrometer scale (Figure S5d). If only hexadecylamine was used as a surfactant, the cores are also large and the nanorods are short, confirmed by SEM studies of $CoCu_{0.05}$ and $CoCu_{0.1}$ (Figure S5e-f).

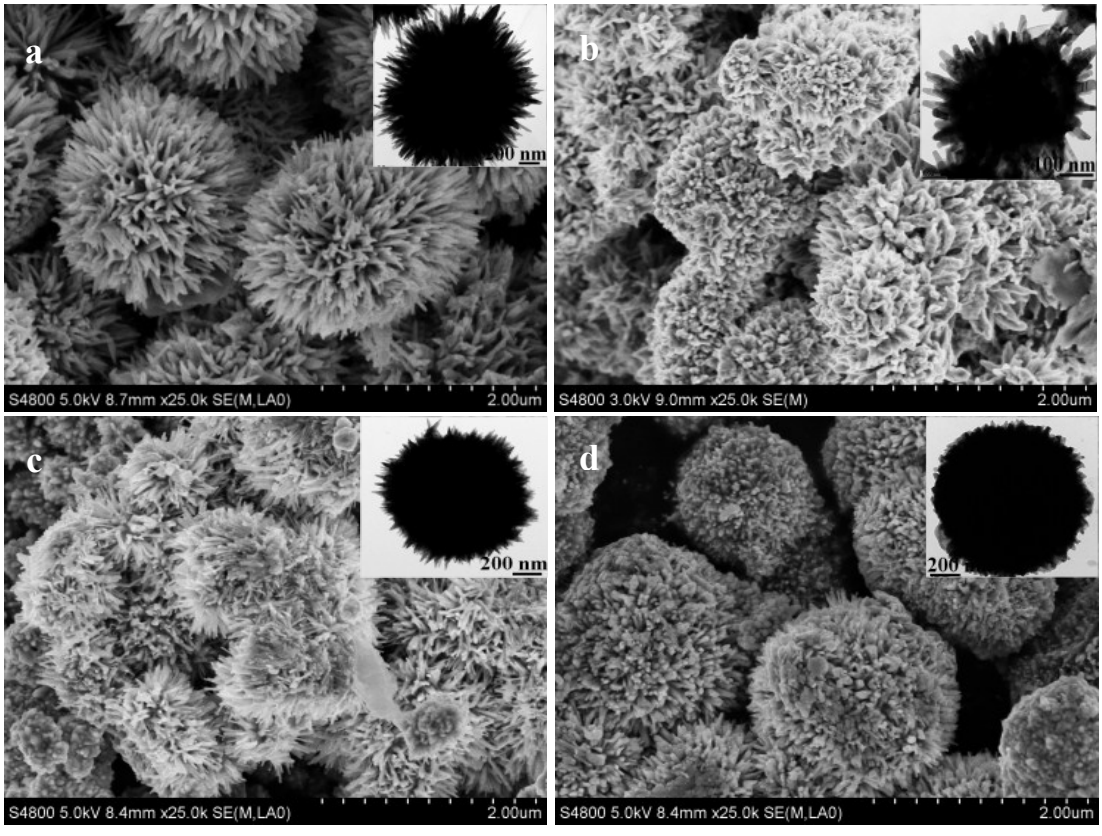

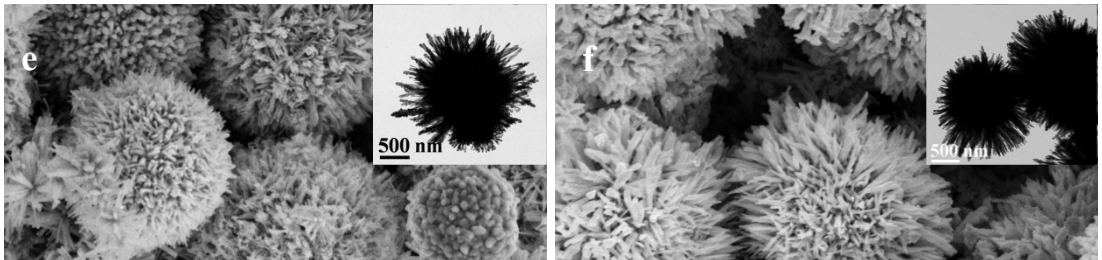

Figure S5. SEM images of (a) $CoCu_{0.01}$, (b) $CoCu_{0.05}$, (c) $CoCu_{0.1}$ and (d) $CoCu_{0.2}$. These samples were synthesized in thepropylene glycolsolvent at 190^{o}C for 5 h using stearic acid as a surfactant. SEM images of (e) $CoCu_{0.05}$ and (f) $CoCu_{0.1}$ synthesized in propylene glycol solvent at 190^{o}C for 5 h using hexadecylamine as a surfactant.Insets are TEM images of corresponding Co-Cu samples.

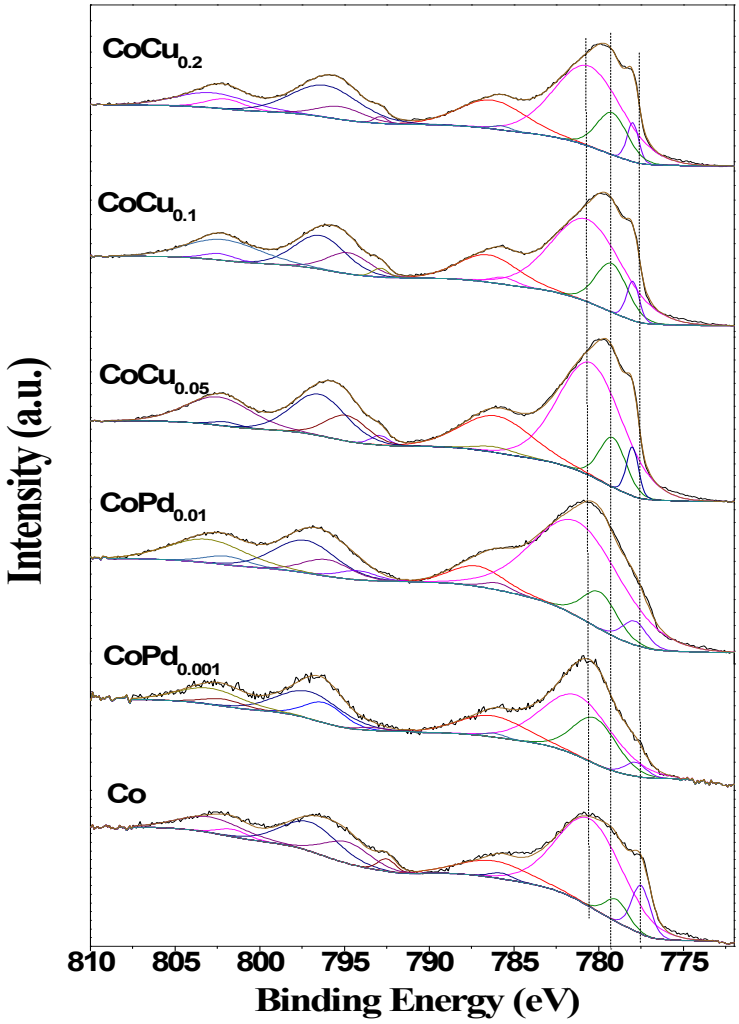

Figure S6. Co 2p electron region of XPS spectra of $CoPd_{0.001}$, $CoPd_{0.01}$, $CoCu_{0.05}$, $CoCu_{0.1}$, and $CoCu_{0.2}$ nanocrystals.

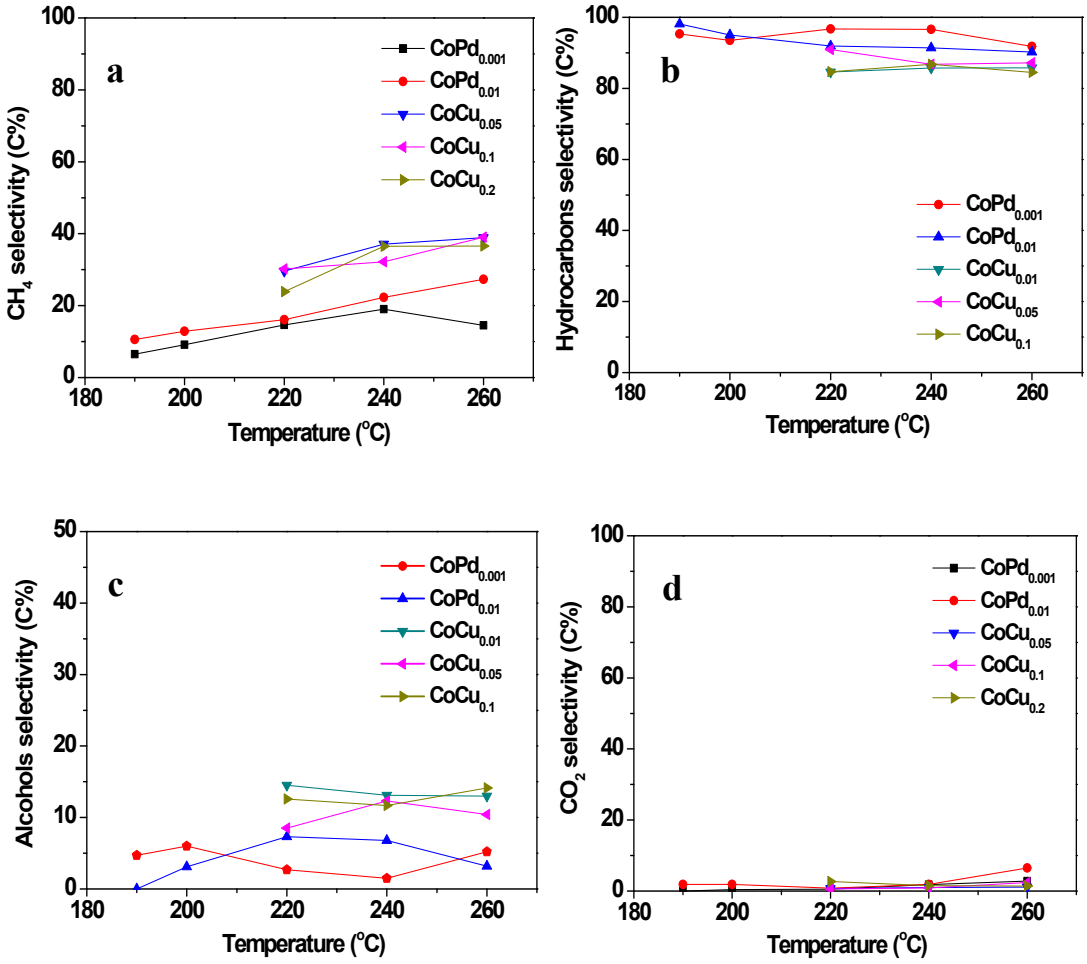

Figure S7. Catalytic performances of Co-Pd and Co-Cu nanocrystals with 1D structure for syngas conversion: (a) CH_4 selectivity, (b) hydrocarbons selectivity, (c) alcohols selectivity and (d) CO_2 selectivity, respectively.

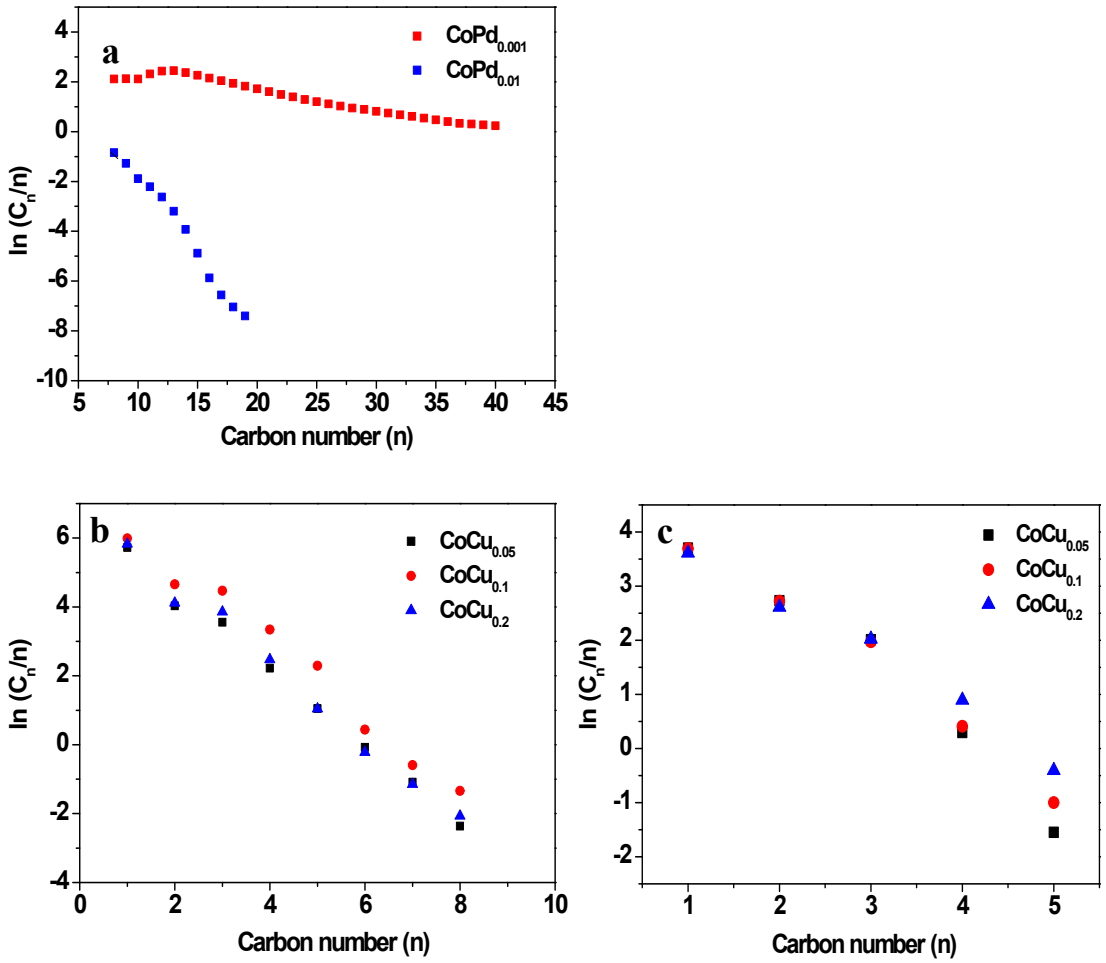

Figure S8. ASF plots based on distribution of hydrocarbons collected at 220°C and 6 MPa over (a) Co-Pd and (b) Co-Cu catalysts. (c)ASF plots based on distribution of alcohols collected at 220°C and 6 MPa over Co-Cu catalysts. (C_n is the carbon molar fraction of the product with carbon number equal to n. C_1-C_7 products were collected in water phase and C_n (n>7) products were collected in the wax and oil phases.) The values of ASF for products chain-lengthening probabilities were calculated according to the following Equation: $C_n / n = \alpha^{n-1}(1-\alpha)^2$

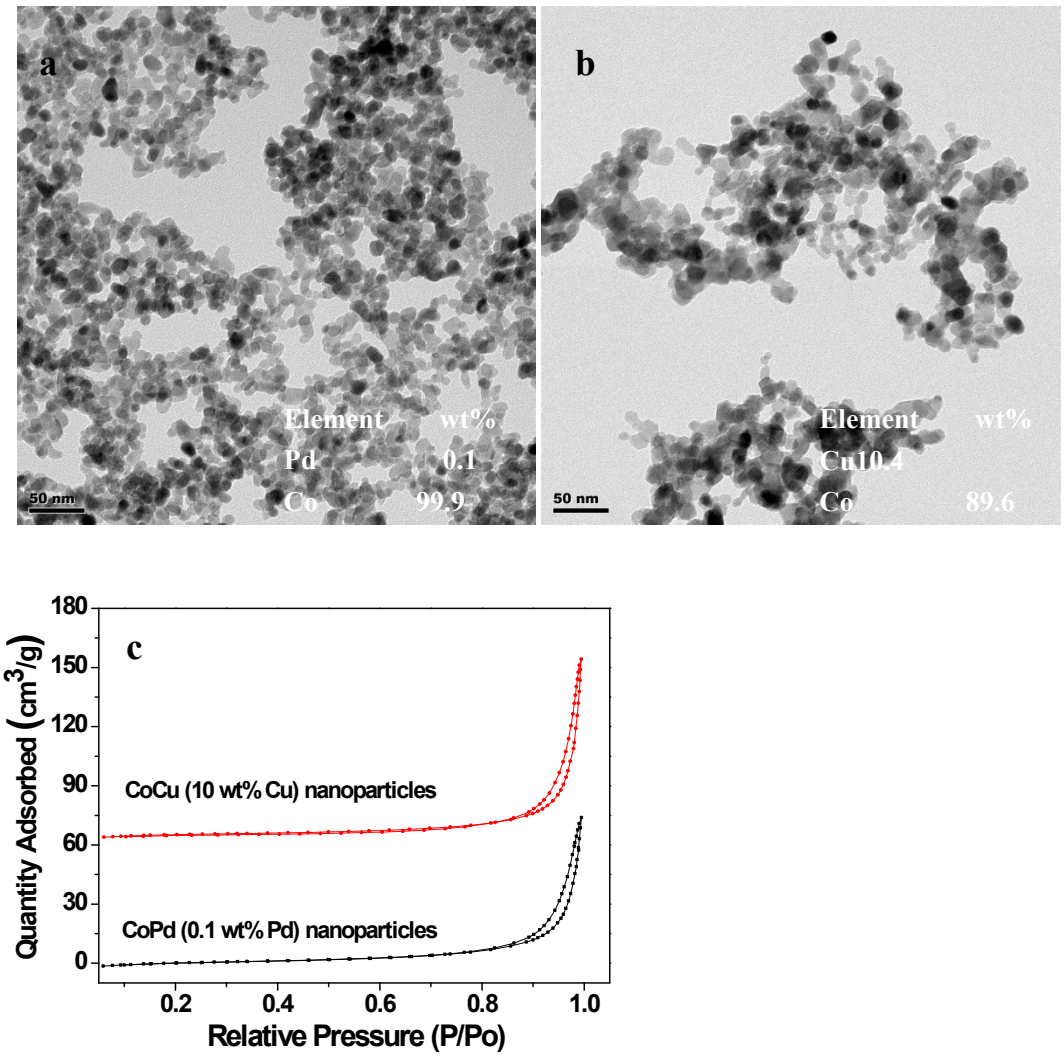

Figure S9. TEM images and corresponding ICP analysis of (a) CoPd (0.1wt% Pd) and (b) CoCu (10wt% Cu) nanoparticlesprepared using the coprecipitation methods.(c) N_2absorption isotherms of CoPd (0.1wt% Pd) and CoCu (10wt% Cu) nanoparticlesprepared using the coprecipitation methods.

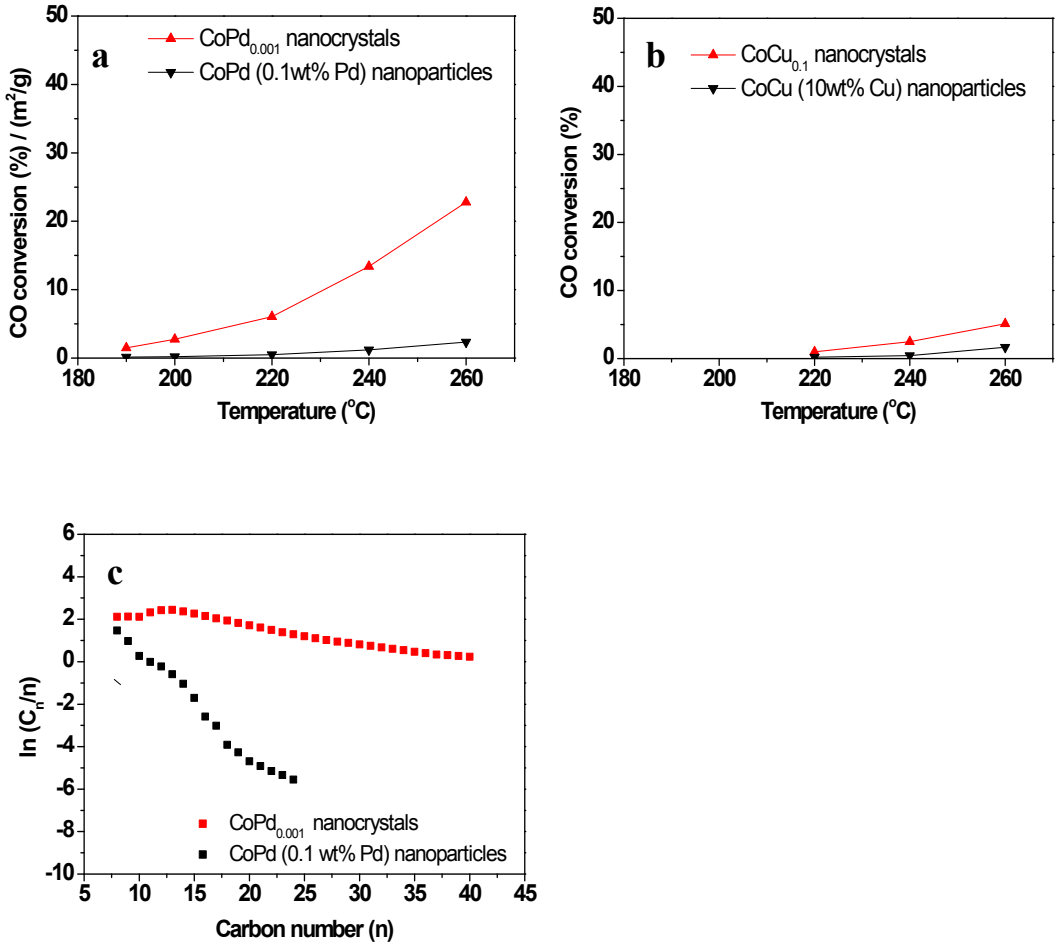

Figure S10. (a)Comparison of catalytic activity per unit surface area of $CoPd_{0.001}$ nanocrystals and CoPd (0.1wt% Pd) nanoparticles.(b) Comparison of catalytic activity per unit surface area of $CoCu_{0.1}$ nanocrystals and CoCu (10wt% Cu) nanoparticles.(c) ASF plots based on distribution of hydrocarbons collected at 220°C and 6 MPa over $CoPd_{0.001}$ nanocrystals and CoPd (0.1wt% Pd) nanoparticles.(These nanoparticles were prepared via coprecipitation methods.)

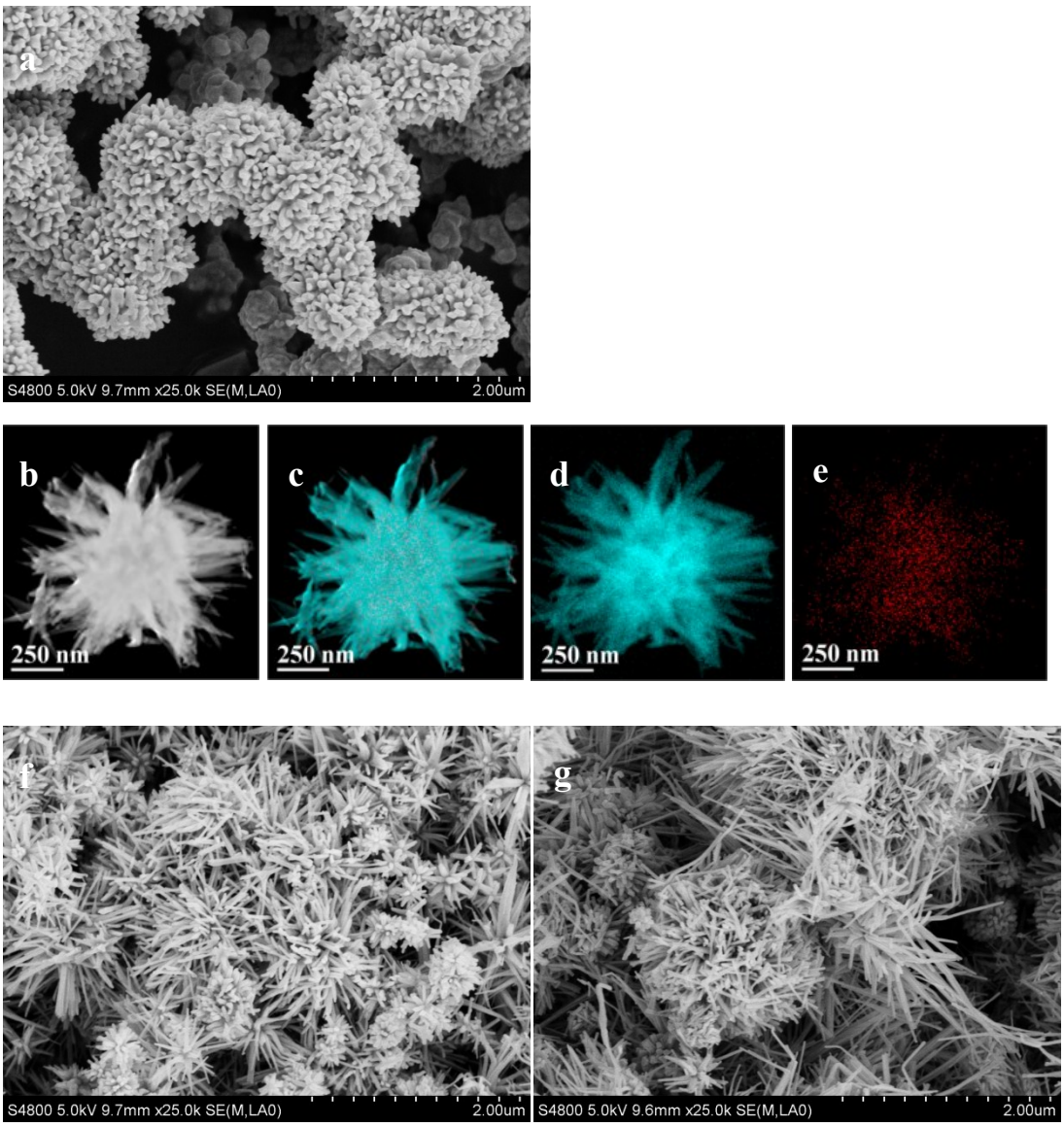

Figure S11. (a) SEM image of $CoPd_{0.01}$, (b) Bright-field TEM image of $CoPd_{0.01}$, and (c-e) the corresponding element maps of Co (blue) and Pd (red) in $CoPd_{0.01}$ after catalytic tests (220^{o}C, 6MP, 24 hr). SEM images of (f) $CoCu_{0.05}$ and (g) $CoCu_{0.2}$ catalysts after catalytic tests (220^{o}C, 6MP, 24 hr).

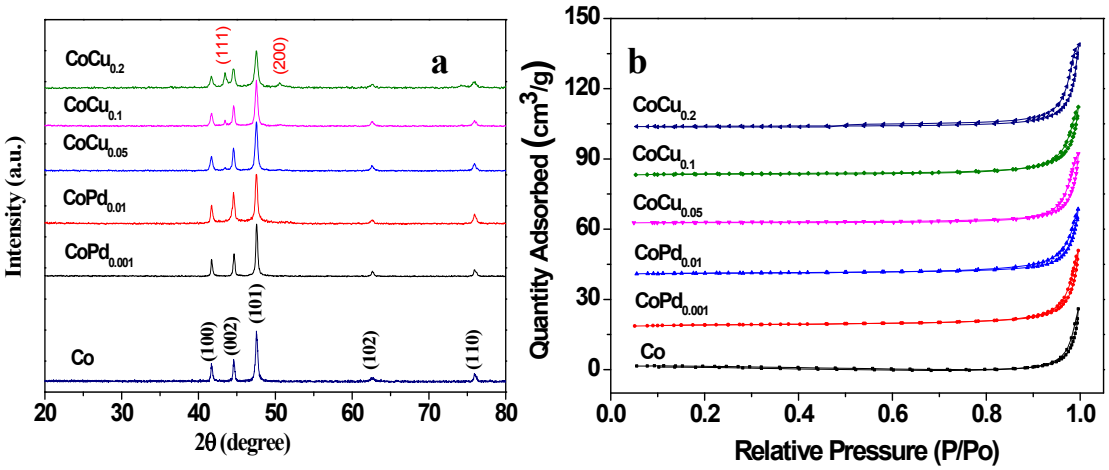

Figure S12. (a) XRD patterns and (b) N_2 absorption isotherms of Co-based nanocrystals after catalytic tests (220°C, 6MP, 24 hr).

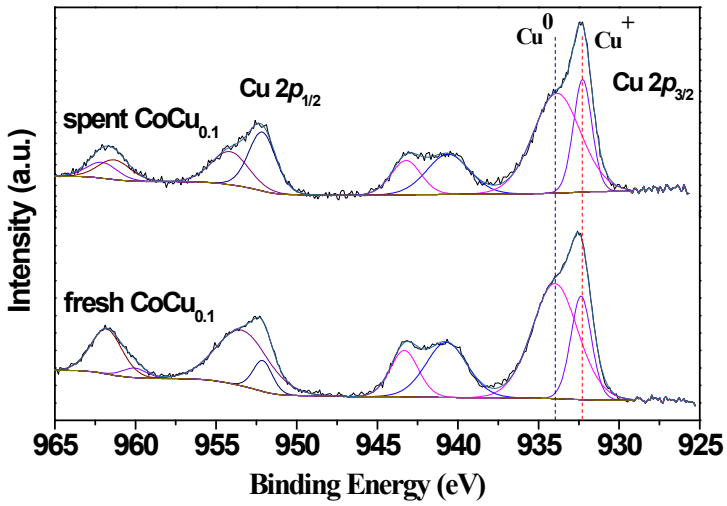

Figure S13. Cu 2p electron region of XPS profiles of fresh and spent $CoCu_{0.1}$.

1. Supporting Tables

Table S1. The exact chemical compositions of Co-Pd and Co-Cu nanocrystals (including fresh and spent ones) were determinedby ICP. The surface compositions of Co-Pd and Co-Cu nanocrystals (including fresh and spent ones) were determined by XPS.

Sample	Pd or Cu (wt%) by ICP	Pd or Cu (wt%) by XPS
fresh $CoPd_{0.001}$	0.1	1.1
fresh $CoPd_{0.01}$	0.9	5.3
fresh $CoCu_{0.05}$	5.1	26.3
fresh $CoCu_{0.1}$	9.2	27.6
fresh $CoCu_{0.2}$	19.6	29.8
spent $CoPd_{0.001}$	0.1	0.9
spent $CoPd_{0.01}$	1.0	2.7
spent $CoCu_{0.05}$	5.3	7.9
spent $CoCu_{0.1}$	10.7	6.9
spent $CoCu_{0.2}$	20.3	9.5

Table S2. Surface areas of fresh and spent Co-based bimetallic catalysts detected by N_2 sorption isotherms[a].

Sample	S_{BET}（m^2/g)
fresh $CoPd_{0.001}$	2.3
fresh $CoPd_{0.01}$	1.7
fresh $CoCu_{0.05}$	7.6
fresh $CoCu_{0.1}$	10.7
fresh $CoCu_{0.2}$	7.1
fresh CoPd[b]	17.6
fresh CoCu[b]	15.7
spent $CoPd_{0.001}$	2.7
spent $CoPd_{0.01}$	1.9
spent $CoCu_{0.05}$	6.1
spent $CoCu_{0.1}$	5.7
spent $CoCu_{0.2}$	4.6

[a] surface area: BET method; [b] catalyst preparation: coprecipitation methods.

Table S3. Catalytic result of $CoPd_{0.001}$ nanocrystals for syngas conversion

Temp.. (℃)	CO Conv. (%)	CH_4 Sel. (C%)	C_{2+} Sel. (C%)	C_{5+} Sel. (C%)
190	8.8	6.5	88.8	78.42
200	11.6	9.1	84.7	74.61
220	22.4	14.6	82.2	69.58
240	43.5	19.0	77.64	57.85
260	71.2	14.5	77.5	66.4

T/℃	Selectivity(C %)			ROH distribution(wt%)					RH distribution(wt%)				
	ROH	RH	CO_2	MeOH	EtOH	PrOH	BuOH	C_{5+}OH	C_1	C_2	C_3	C_4	C_{5+}
190	4.7	95.3	0	19.1	15.8	10.0	17.8	37.0	11.4	3.1	7.2	6.0	72.2
200	6.0	93.5	0.4	19.4	13.0	7.4	6.6	53.4	21.6	4.5	9.4	7.7	56.6
220	2.7	96.7	0.5	30.5	13.8	6.6	4.0	45.0	11.3	3.1	7.1	5.9	72.4
240	1.5	96.6	1.8	38.8	16.8	18.1	2.5	23.6	25.4	6.4	10.0	7.6	50.4
260	5.2	91.8	2.8	31.6	20.1	7.5	12.0	28.2	19.0	4.5	5.49	3.3	67.5

Table S4. Catalytic result of $CoPd_{0.01}$ nanocrystals for syngas conversion

Temp.. (℃)	CO Conv. (%)	CH_4 Sel. (C%)	C_{2+} Sel. (C%)	C_{5+} Sel. (C%)
190	3.4	10.6	87.5	72.9
200	6.3	12.9	82.1	64.9
220	13.9	16.1	75.8	54.6
240	30.8	22.3	69.1	48.1
260	52.4	27.3	62.9	45.1

T/℃	Selectivity(C %)			ROH distribution(wt%)					RH distribution(wt%)				
	ROH	RH	CO_2	MeOH	EtOH	PrOH	BuOH	C_{5+}OH	C_1	C_2	C_3	C_4	C_{5+}
190	trace	98.1	1.9	trace	trace	trace	trace	trace	34.6	11.4	19.1	12.2	22.7
200	3.1	95.0	1.9	67.1	15.8	9.5	5.9	1.7	36.5	11.9	19.5	12.3	19.7
220	7.3	91.9	0.8	64.0	18.2	6.2	4.3	7.3	31.8	10.3	16.2	11.6	29.9
240	6.8	91.4	1.9	68.3	17.2	5.6	3.6	5.29	68.3	17.2	5.6	3.6	1.9
260	3.2	90.2	6.5	74.1	17.8	5.1	2.5	0.5	74.1	17.8	5.1	2.5	0.5

Table S5. Catalytic result of $CoCu_{0.05}$ nanocrystals for syngas conversion

Temp.. (℃)	CO Conv. (%)	CH_4 Sel. (C%)	C_{2+} Sel. (C%)	C_{5+} Sel. (C%)
220	4.7	29.6	55	29.9
240	9.8	37.1	48.6	14.2
260	29.4	38.9	46.9	5.7

T/℃	Selectivity(C %)			ROH distribution(wt%)					RH distribution(wt%)				
	ROH	RH	CO_2	MeOH	EtOH	PrOH	BuOH	$C_{5+}OH$	C_1	C_2	C_3	C_4	C_{5+}
220	14.5	84.6	0.7	49.7	26.9	18.5	4.4	0.5	54.1	18.8	17.7	6.1	3.4
240	13.1	85.7	1	47.1	26.9	19.3	5.4	1.2	52.9	20.2	18.2	6.8	1.9
260	13	85.8	1.1	47.6	26.7	19.2	5.3	1.2	47.7	17.5	17.5	11.2	6.1

Table S6. Catalytic result of $CoCu_{0.1}$ nanocrystals for syngas conversion

Temp.. (℃)	CO Conv. (%)	CH_4 Sel. (C%)	C_{2+} Sel. (C%)	C_{5+} Sel. (C%)
220	10.5	30.2	60.7	15.7
240	26.6	32.2	54.6	9.1
260	54.7	39	48.2	13.0

T/℃	Selectivity(C %)			ROH distribution(wt%)					RH distribution(wt%)				
	ROH	RH	CO_2	MeOH	EtOH	PrOH	BuOH	$C_{5+}OH$	C_1	C_2	C_3	C_4	C_{5+}
220	8.5	90.9	0.6	50.3	27.4	16.8	2.6	2.9	40.2	19.8	24.2	10.3	5.5
240	12.3	86.8	0.9	52.8	23.9	14.6	3.6	5.1	40.0	16.1	21.0	14.1	8.7
260	10.4	87.2	2.4	50.3	23.8	13.4	6.1	6.5	48.4	15.5	17.0	7.5	11.6

Table S7. Catalytic result of $CoCu_{0.2}$ nanocrystals for syngas conversion

Temp.. (℃)	CO Conv. (%)	CH_4 Sel. (C%)	C_{2+}Sel. (C%)	C_{5+} Sel. (C%)
220	3.3	23.9	60.8	50.0
240	7.3	36.5	50.3	22.2
260	32.1	36.6	47.9	9.6

T/℃	Selectivity(C %)			ROH distribution(wt%)					RH distribution(wt%)				
	ROH	RH	CO_2	MeOH	EtOH	PrOH	BuOH	$C_{5+}OH$	C_1	C_2	C_3	C_4	C_{5+}
220	12.6	84.7	2.7	46.5	24.4	20.0	6.9	2.2	51.9	17.6	19.9	6.6	4.1
240	11.7	86.8	1.5	51.9	24.5	16.2	5.9	1.5	49.6	17.2	20.7	8.5	4.0
260	14.1	84.5	1.4	48.8	24.0	17.2	6.4	3.7	44.2	16.9	20.2	9.9	8.8

Table S8. Catalytic result of Co nanocrystals for syngas conversion

Temp. (℃)	CO Conv. (%)	CH_4 Sel. (C%)	C_{2+}Sel. (C%)	C_{5+} Sel. (C%)
190	2.9	5.3	94.7	87.7
200	3.6	5.3	92.5	83.9
220	10.6	14.9	82.0	73.8
240	14.6	22.8	71.7	58.9

260	25.8	27.6	67.5	48.8

T/℃	Selectivity(C %)			ROH distribution(wt%)					RH distribution(wt%)				
	ROH	RH	CO_2	MeOH	EtOH	PrOH	BuOH	$C_{5+}OH$	C_1	C_2	C_3	C_4	C_{5+}
190	trace	100	0	trace	trace	trace	trace	trace	27.6	6.1	14.0	11.8	40.3
200	1.7	97.8	0.4	77.0	10.8	4.7	5.2	2.0	29.1	8.2	15.0	12.0	35.5
220	1.6	96.9	1.4	51.6	11.2	4.8	5.5	26.7	35.3	4.8	8.0	6.5	45.2
240	3.6	94.5	1.8	59.2	14.6	6.3	5.8	13.9	39.8	5.99	8.4	6.7	38.9
260	2.1	95.1	2.7	67.3	15.5	4.8	3.6	8.6	35.6	6.5	8.9	7.9	40.9

Table S9. Catalytic result of CoPd (0.1 wt% Pd) nanoparticles prepared using coprecipitation method for syngas conversion

Temp. (℃)	CO Conv. (%)	CH_4 Sel. (C%)	C_{2+}Sel. (C%)	C_{5+} Sel. (C%)
190	2.6	3.8	90.5	71.0
200	3.8	5.4	89.9	67.0
220	8.6	10.3	78.2	50.7
240	21.1	13.8	69.8	51.6
260	41.4	19.6	57.1	41.3

T/℃	Selectivity(C %)			ROH distribution(wt%)					RH distribution(wt%)				
	ROH	RH	CO_2	MeOH	EtOH	PrOH	BuOH	$C_{5+}OH$	C_1	C_2	C_3	C_4	C_{5+}
190	2.0	94.3	3.7	39.5	21.1	11.1	15.6	12.7	11.7	13.5	25.7	16.9	32.1
200	1.5	95.3	3.2	36.2	26.3	13.6	15.3	8.5	13.6	12.7	25.1	18.0	30.6
220	9.9	88.5	1.7	28.8	26.9	10.5	12.6	21.3	19.6	10.6	21.1	16.0	32.6
240	12.1	83.6	4.3	28.2	21.4	11.0	11.3	28.2	31.1	8.6	16.6	13.3	30.3
260	10.3	76.7	13.0	10.3	76.7	13.0	12.7	24.0	39.6	9.2	15.2	11.7	24.4

Table S10. Catalytic result of CoCu (10 wt% Cu) nanoparticles prepared using coprecipitation method for syngas conversion

Temp. (℃)	CO Conv. (%)	CH_4 Sel. (C%)	C_{2+}Sel. (C%)	C_{5+} Sel. (C%)
220	3.2	13.6	70.6	37.8
240	6.8	21	65.5	20.9
260	26.4	26.4	63.3	16.7

T/℃	Selectivity(C %)			ROH distribution(wt%)					RH distribution(wt%)				
	ROH	RH	CO_2	MeOH	EtOH	PrOH	BuOH	$C_{5+}OH$	C_1	C_2	C_3	C_4	C_{5+}
220	11.9	84.2	3.9	48.2	26.1	19.0	5.1	1.5	36.4	19.4	25.5	11.1	7.7
240	10.6	86.5	2.8	39.7	30.0	19.6	8.6	2.1	35.1	17.4	24.6	13.1	9.8

260	8.3	89.7	2.0	37.6	26.4	17.6	8.8	9.5	34.1	16.1	23.4	13.9	12.6

Note: RH: hydrocarbons; ROH: alcohols.